Available on: http://gjetr.ep-journals.org/ E-ISSN: 3051-3782, P-ISSN: 3051-3774

Global Journal of Engineering and Technology Review

Volume: 02 Issue: 11 November 2026

Artificial-Intelligence-Assisted Steam Temperature Control of a Fire-Tube Boiler Supplying Garment Ironing Lines: PSO-Tuned Feedback Combined with Neural Demand-Forecast Feedforward

Nguyen Thi Lan Huong

Department of Electrical Engineering, Faculty of Mechanical and Electrical Engineering, Hanoi Industrial and Trade University, VietNam

Published Date: November 26, 2026 **Article DOI : 10.65150/EP-gjetr/V2E11/2026-11**

ABSTRACT: Small fire-tube boilers that feed the ironing lines of garment factories face abrupt, bell-driven swings in steam demand, and the resulting temperature excursions degrade pressing quality. This study examines which artificial-intelligence (AI) techniques improve steam temperature control in this setting. A nonlinear energy-balance model of a 500 kg/h boiler serving 30 ironing stations was simulated with a stochastic, timetable-driven demand generator. Five controllers were compared: Ziegler–Nichols PID, PID tuned by particle swarm optimisation (PSO), a PSO-tuned fuzzy self-tuning PID, PID with conventional steam-flow feedforward, and PID with feedforward driven by a neural network that forecasts demand 60 s ahead. The network was trained on 40 simulated days, and all controllers were evaluated on 20 unseen days and under two robustness conditions. PSO tuning lowered the mean absolute error (MAE) from 0.280 to 0.244 °C, whereas fuzzy gain scheduling produced no further gain (0.247 °C) because the plant is lag-dominant and nearly linear. Neural predictive feedforward reduced MAE to 0.148 °C (−39 %), cut the largest daily deviation from 2.29 to 0.91 °C (−60 %) and kept the temperature within ±0.5 °C for 97.5 % of the shift. Fuel use was unchanged (differences of about 0.1 %), and an unannounced five-minute timetable shift removed most of the peak-deviation benefit. For garment-factory boilers, the value of AI lies in anticipating scheduled load changes rather than in making the feedback law more elaborate; the benefit is steam-quality stability, not fuel saving. All results are simulation-based and require plant validation.

KEYWORDS: steam boiler, garment industry, ironing, temperature control, particle swarm optimisation, fuzzy PID, neural network forecasting, feedforward control

INTRODUCTION

Steam is the working medium of garment finishing. Irons, vacuum pressing tables and form finishers all draw saturated steam from a central boiler, and the temperature and dryness of that steam determine how well creases are set and whether water spots appear on the fabric. The energy involved is not trivial: reviews of the textile and apparel sector document its heavy use of thermal energy and the range of efficiency measures available for steam systems (Hasanbeigi & Price, 2012), and a recent gate-to-gate assessment of ready-made garment production lists steam generation among the areas with saving potential (Uddin et al., 2024).

The boilers concerned are small. Documented factory audits describe a 0.5 t/h wood-fired unit delivering steam at 6 bar and 165 °C to 30 ironing stations (Geres, 2024) and a 0.5 t/h diesel fire-tube unit serving about 50 steam ironing units (UNIDO, 2020). Such units are normally run by a pressure switch or a single-loop PID controller acting on the firing rate. The control problem they face is unusual in one respect: the load is set by people working to a timetable. When the break bell rings, most stations stop drawing steam within a minute; when work resumes, demand returns just as quickly. Between these events the load fluctuates randomly as individual operators start and stop. A feedback controller can respond only after the temperature has already moved, and the combustion and heat-transfer lags of the boiler then limit how fast the deviation can be corrected.

Artificial-intelligence methods have been applied widely to boiler control, mostly in power generation, and typically in the form of fuzzy or neural self-tuning of the PID gains, metaheuristic tuning, or reinforcement learning. It is less clear which of these techniques is useful for a small saturated-steam boiler whose difficulty is not strong nonlinearity but an unmeasured and partly predictable disturbance. A technique that works well on a superheater with a large dead time may bring little to a lag-dominant fire-tube shell.

This paper addresses that question by simulation. Its objectives are: (i) to build a compact dynamic model of a fire-tube boiler supplying a 30-station ironing line, together with a realistic stochastic model of the steam demand over a working day; (ii) to compare, on equal terms, a conventional PID controller, a PSO-tuned PID controller and a PSO-tuned fuzzy self-tuning PID controller; (iii) to design and test a feedforward scheme in which a small neural network forecasts steam demand one minute ahead from the shift timetable and the measured steam flow; and (iv) to quantify the robustness of each scheme to plant mismatch and to an unannounced change in the timetable. The research questions are whether intelligent feedback tuning improves on a well-tuned PID controller for this class of plant, and how much additional benefit can be obtained by forecasting the load.

License: This is an open access article under the CC BY 4.0 license: https://creativecommons.org/licenses/by/4.0/

LITERATURE REVIEW

Boiler dynamics and conventional control

The reference description of boiler dynamics is the drum-boiler model of Åström and Bell (2000), which derives a low-order nonlinear model from mass and energy balances and shows that the stored energy in water, steam and metal governs the pressure response. For fire-tube boilers, Gutiérrez Ortiz (2011) developed a first-principles dynamic model, and Tognoli et al. (2018) built a detailed dynamic model of an industrial fire-tube boiler, tuned a PID pressure controller for it and studied its behaviour under several variable steam-demand profiles. These studies establish that, for saturated-steam shells, steam temperature and pressure are tied through the saturation curve and that the dominant dynamics are a large thermal capacitance in series with comparatively short combustion and heat-transfer lags.

PID control remains the industrial standard for this loop. The classical reaction-curve rules of Ziegler and Nichols (1942) are still widely used for commissioning, although they are known to give aggressive settings for lag-dominant processes; model-based rules such as those of Skogestad (2003) and the design methods collected by Åström and Hägglund (2006) offer better trade-offs between performance and robustness. Feedforward from a measured disturbance is the standard remedy when feedback alone is too slow (Seborg et al., 2016).

Fuzzy and metaheuristic approaches

Fuzzy logic (Zadeh, 1965) entered process control through the linguistic controller of Mamdani and Assilian (1975) and the functional rule consequents of Takagi and Sugeno (1985). Two early schemes used fuzzy inference to adapt PID gains online: the fuzzy self-tuning controller of He et al. (1993) and the fuzzy gain scheduling of Zhao et al. (1993). These ideas have been reused extensively for boiler steam-temperature loops, where simulation studies usually report faster and better-damped responses than fixed-gain PID control.

Particle swarm optimisation (Kennedy & Eberhart, 1995), with the inertia weight of Shi and Eberhart (1998) and the convergence analysis of Clerc and Kennedy (2002), has become a common tool for tuning such controllers. Aygun et al. (2012) applied a PSO-tuned PID controller to the bed temperature of a circulating fluidised-bed boiler and compared it with a fuzzy logic controller at several loads. Ait Sahed et al. (2015) combined PSO with fuzzy predictive control and evaluated it on a multivariable industrial boiler model. Mien et al. (2020) used PSO to optimise the scaling coefficients of a fuzzy-PID controller for the temperature of a resistance furnace, a thermal process with dynamics comparable to those studied here.

Neural networks and reinforcement learning

Neural networks trained by back-propagation (Rumelhart et al., 1986) have been used both as models and as gain tuners. Liu et al. (2024) implemented a back-propagation neural network self-tuning PID controller for steam drum pressure and reported smaller static deviation and maximum error than conventional PID control. Reinforcement learning has been explored more recently: Zhan et al. (2022) trained a combustion-optimisation policy for thermal power units entirely from historical data; Lee and Jung (2024) combined an internal-model-control PID controller with a deep deterministic policy gradient agent for ship oil-fired boilers; and Okafor and Alowaifeer (2025) fused deep reinforcement learning, model-reference adaptive control and optimised PID control for drum-boiler pressure regulation.

Research gap

Three gaps emerge. First, almost all of this work concerns utility or large industrial boilers; small boilers serving garment finishing, whose load is dominated by a human work schedule, have received little attention from the control community. Second, intelligent feedback controllers are frequently compared only with a Ziegler–Nichols PID controller, which is a weak baseline; it is then unclear whether the reported benefit comes from the intelligent structure or simply from better tuning. Third, the predictable part of the load, which in a garment factory is known in advance from the timetable, is rarely exploited. The present study addresses all three by using an optimally tuned PID controller as the baseline for every comparison and by testing a learning-based forecast of the load as a feedforward signal.

MATERIALS AND METHODS

Research design

The study is a simulation experiment. A nonlinear boiler model and a stochastic demand model were implemented in Python (NumPy and Numba), five control schemes were tuned or trained on one set of data, and all were then evaluated on data not used for tuning. Figure 1 shows the structure of the proposed scheme. No measurements from an operating factory were used; the plant size and steam conditions were taken from published factory audits (Geres, 2024; UNIDO, 2020).

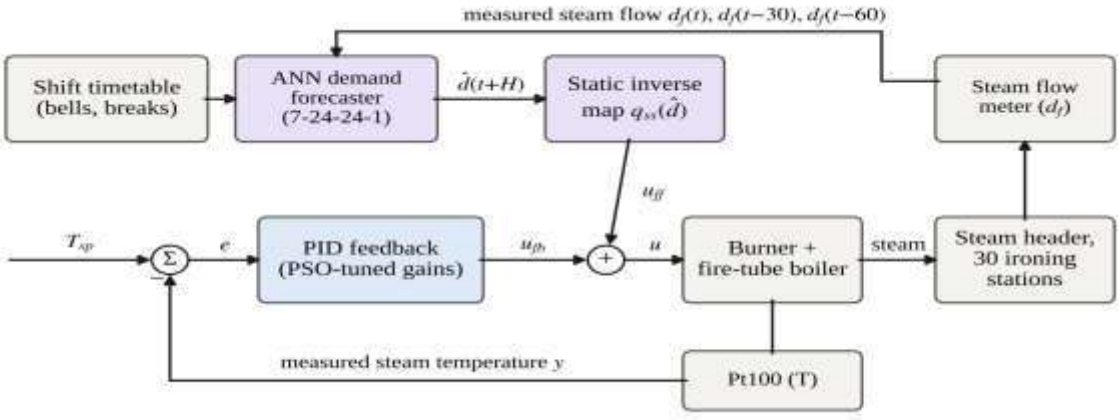

Figure 1. Structure of the proposed control scheme: PSO-tuned PID feedback with neural demand-forecast feedforward.

License: This is an open access article under the CC BY 4.0 license: https://creativecommons.org/licenses/by/4.0/

Boiler model

The boiler is a 500 kg/h fire-tube unit producing saturated steam at a nominal 165 °C (about 7.0 bar absolute). Feedwater level is assumed to be held constant by its own controller, so the water inventory is fixed and the steam and water are in saturation equilibrium at temperature T. The energy balance is

$$C \cdot \mathrm{d}T/\mathrm{d}t = \eta(q_a) \cdot Q_{max} \cdot q_w - m_s \cdot (h_g - h_{fw}) - UA \cdot (T - T_{amb}) \qquad (1)$$

where C is the effective heat capacity of water and metal, Q_{max} the rated fuel power, q_w the normalised heat flux reaching the water, m_s the steam mass flow, h_g and h_{fw} the enthalpies of saturated vapour and feedwater (Wagner & Pruß, 2002), and UA the shell loss coefficient. The firing command $u \in [0, 1]$ passes through a slew limit of 5 %/s, a transport delay θ, a burner lag and a gas-side/tube-wall lag:

$$\tau_a \cdot \mathrm{d}q_a/\mathrm{d}t = u(t - \theta) - q_a, \quad \tau_w \cdot \mathrm{d}q_w/\mathrm{d}t = q_a - q_w \qquad (2)$$

Combustion efficiency varies mildly with firing rate, $\eta(q_a) = \eta_0 - 0.08\,(q_a - 0.6)^2$. The stations draw steam through fixed restrictions, so the flow scales with header pressure:

$$m_s = d(t) \cdot p_{sat}(T) / p_{sat}(165\ °C), \quad d(t) = 30 + 12 \cdot n(t)\ \ [\mathrm{kg/h}] \qquad (3)$$

where $n(t)$ is the number of stations in use, 12 kg/h is the consumption of one working station and 30 kg/h represents distribution losses and traps. Saturation pressure is computed from the Antoine equation, $\log_{10} p\ [\mathrm{mmHg}] = 8.14019 - 1810.94 / (244.485 + T\ [°\mathrm{C}])$. The temperature is measured by a sheathed sensor with a first-order lag τ_s and additive Gaussian noise of standard deviation 0.03 °C. Table 1 lists the parameter values. The model is integrated by the explicit Euler method with a step of 0.5 s; the controllers run with a sampling period of 1 s.

Table 1. Parameters of the boiler and ironing-line model.

Parameter	Value
Effective heat capacity of water and metal, C	5670 kJ/K
Rated fuel power, Q_{max}	420 kW
Peak efficiency, η_0	0.87
Shell loss coefficient, UA	0.030 kW/K
Ambient temperature, T_{amb}	30 °C
Saturated-vapour enthalpy at 165 °C, h_g	2763 kJ/kg
Feedwater enthalpy at 60 °C, h_{fw}	251 kJ/kg
Burner lag, τ_a	12 s
Gas-side/tube-wall lag, τ_w	40 s
Transport delay, θ	15 s
Sensor lag, τ_s	8 s
Measurement noise (standard deviation)	0.03 °C
Number of ironing stations	30
Steam per working station	12 kg/h
Distribution losses and traps	30 kg/h

A 5 % step in firing rate at the nominal operating point (18 stations in use) gave a reaction curve that was fitted by the two-point method to a first-order-plus-dead-time model with gain $K = 82.2$ °C per unit firing rate, time constant $\tau = 1242$ s and apparent dead time $\theta_{app} = 79$ s. The ratio $\theta_{app}/\tau \approx 0.06$ shows that the process is strongly lag-dominant.

Steam demand model

A working day runs from 07:00 to 16:40. Work periods are 07:30–09:30, 09:40–11:30, 12:30–14:30 and 14:40–16:30, giving four start bells and four stop bells. On each simulated day the number of staffed stations is drawn uniformly from 24 to 30, and each bell is displaced from its nominal time by a normally distributed error with a standard deviation of 20 s. After a start bell every staffed station begins work after a gamma-distributed delay (shape 2, mean 50 s). During a work period each station alternates between working and idle states as a two-state Markov chain with mean dwell times of 240 s and 60 s, which gives an average utilisation of 80 %. After a stop bell each working station finishes after an exponentially distributed time with a mean of 20 s. The steam flow meter is modelled with 2 % multiplicative noise and a 5 s first-order filter. Seventy days were generated: 40 for training, 10 for validation and 20 for testing.

Feedback controllers

All feedback controllers share the same structure,

$$u_{fb}(k) = K_p \cdot e(k) + I(k) - K_d \cdot \Delta y_f(k)/T_s, \quad I(k+1) = I(k) + K_i \cdot e(k) \cdot T_s \qquad (4)$$

with $e = T_{sp} - y$, derivative action on the measurement filtered with a 10 s time constant, output limits of 0 and 1, and conditional integration as anti-windup. Three sets of gains were considered.

ZN-PID. Gains from the Ziegler–Nichols reaction-curve rules applied to the identified model: $K_p = 1.2\tau/(K\theta_{app})$, $T_i = 2\theta_{app}$, $T_d = 0.5\theta_{app}$.

PSO-PID. The three gains were found by PSO on a benchmark scenario consisting of a 150 → 165 °C set-point step at nominal load, followed by a load increase of ten stations and a load decrease of 18 stations. The cost was

$$J = (1/3)\,\Sigma_j\, \mathrm{ITAE}_j/\mathrm{ITAE}_j^{ZN} + 0.3 \cdot \mathrm{TV}/\mathrm{TV}^{ZN} + 2 \cdot \max(0, M_p - 0.5) \qquad (5)$$

where the sum runs over the three segments of the scenario, ITAE is the integral of time-weighted absolute error with time restarted at each event, TV is the total variation of the control signal (a measure of actuator wear), M_p is the set-point overshoot in °C, and the superscript ZN denotes the value obtained with the ZN-PID controller. The swarm had 40 particles and ran for 100 iterations with an inertia weight decreasing linearly from 0.9 to 0.4 and acceleration coefficients of 1.49; ten independent runs were made.

License: This is an open access article under the CC BY 4.0 license: https://creativecommons.org/licenses/by/4.0/

PSO-FPID. A fuzzy self-tuning PID controller in the spirit of He et al. (1993) and Zhao et al. (1993) adjusts the gains at every sample:

$$K_x = K_{x0} \cdot (1 + \alpha_x \cdot \Delta K_x(E, EC)), \quad x \in \{p, i, d\} \qquad (6)$$

The inputs $E = K_e \cdot e$ and $EC = K_{ec} \cdot de/dt$ are clipped to [−1, 1] and fuzzified by seven triangular membership functions (NB to PB) that form a partition of unity (Figure 2a). Inference is of the zero-order Takagi–Sugeno type with product conjunction and weighted-average defuzzification over 49 rules for each gain. The rule consequents (Figure 2b–d) encode three heuristics: raise the proportional gain when the error is large or growing and lower it when the error is shrinking; suppress integral action for large errors and strengthen it near the set-point; and add derivative action when the output approaches the set-point quickly. With i and $j \in \{-3, \ldots, 3\}$ denoting the indices of the E and EC labels and $s = \mathrm{sign}(i \cdot j)$, the consequents are $\Delta K_p = \mathrm{clip}(|i| - 1 + s)$, $\Delta K_i = \mathrm{clip}(3 - 2|i| - [|j| \geq 2])$ and $\Delta K_d = \mathrm{clip}(\min(|i|, |j|) \cdot [s < 0] - [s > 0])$, clipped to ±3 and divided by 3. Eight parameters (K_{p0}, K_{i0}, K_{d0}, K_e, K_{ec}, α_p, α_i, α_d) were optimised by PSO with the same cost and settings as for PSO-PID. Because the fixed-gain controller is the special case $\alpha = 0$, one particle of each swarm was initialised at the PSO-PID optimum, so that the fuzzy controller could not finish with a higher cost than the fixed-gain controller.

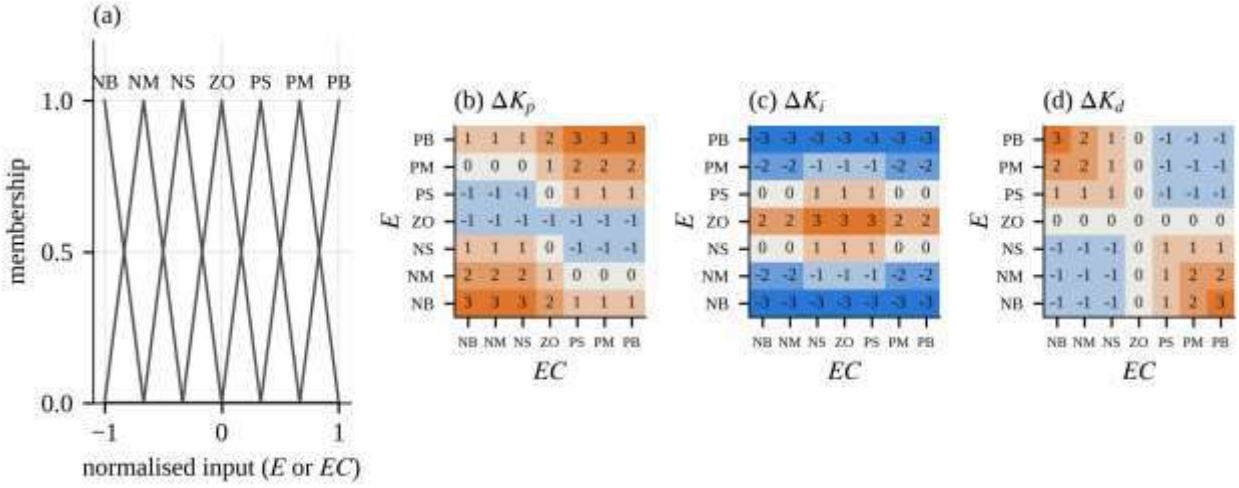

Figure 2. Fuzzy self-tuning PID controller: (a) input membership functions; (b)–(d) rule consequents for the three gain corrections on a scale from −3 (NB) to 3 (PB).

Feedforward schemes

Both feedforward schemes add a term u_{ff} to the PSO-PID output and leave its gains unchanged, so that any difference in performance can be attributed to the feedforward signal alone. The term is obtained from the static inverse of Equations 1 and 3, that is, the firing rate $q_{ss}(d)$ that holds 165 °C at demand d under nominal parameters.

PID+FF. Conventional feedforward uses the filtered steam-flow measurement: $u_{ff}(t) = q_{ss}(d_f(t))$.

PID+ANN-FF (proposed). A multilayer perceptron forecasts the demand H seconds ahead and the forecast replaces the measurement: $u_{ff}(t) = q_{ss}(\hat{d}(t + H))$. The network has seven inputs: the filtered flow now, 30 s ago and 60 s ago; the time to the next scheduled bell and the time since the last one (both clipped at 10 min); a flag indicating whether the next bell is a stop bell; and a flag indicating whether the timetable is currently in a work period. The timetable inputs use the nominal bell times only. Two hidden layers of 24 tanh units feed a linear output. The target is the true demand at $t + H$, smoothed by a 21 s centred moving average. Training used 278,400 samples (40 days sampled every 5 s) and the Adam optimiser (Kingma & Ba, 2015) as implemented in scikit-learn (Pedregosa et al., 2011), with early stopping on a 10 % hold-out. Networks were trained for H = 30, 45, 60, 75 and 90 s, and the horizon was chosen by the closed-loop mean absolute error on the ten validation days.

Evaluation procedure and metrics

Three experiments were run. (1) The benchmark scenario was repeated with 20 measurement-noise sequences different from the one used for tuning; rise time, overshoot, settling time into a ±0.5 °C band, maximum deviation, integral of absolute error (IAE) and TV were recorded. (2) Each controller was run on the 20 test days with the set-point fixed at 165 °C; the mean absolute error (MAE), root-mean-square error (RMSE), maximum deviation, fraction of time within ±0.5 °C and ±1.0 °C, TV and fuel energy were computed over 07:30–16:40. Paired differences between controllers were tested with the Wilcoxon signed-rank test. (3) Robustness was tested on the same 20 days under (a) plant mismatch, with efficiency η_0 reduced from 0.87 to 0.78, heat capacity reduced by 15 % and transport delay increased from 15 to 25 s while the controllers and the feedforward map were left unchanged, and (b) an unannounced timetable change in which the morning break started and ended 5 min later than the timetable known to the forecaster.

RESULTS

Controller tuning

Table 2 gives the controller parameters. The ten PSO runs for the PID gains converged to final costs between 0.8988 and 0.9000, against 1.98 for ZN-PID (Figure 3). For the fuzzy controller the best of ten runs reached a cost of 0.8938, which is 0.6 % below the PSO-PID optimum; the optimiser set α_p and α_d to zero and α_i to 0.10.

License: This is an open access article under the CC BY 4.0 license: https://creativecommons.org/licenses/by/4.0/

Table 2. Controller parameters and tuning cost.

Controller	K_p (1/°C)	K_i (10^{-3}/(°C·s))	K_d (s/°C)	T_i (s)	T_d (s)	Cost J
ZN-PID	0.229	1.45	9.06	158	39.5	1.985
PSO-PID	0.343	2.21	10.41	155	30.4	0.8988
PSO-FPID (base gains)	0.344	2.27	10.46	152	30.4	0.8938

Gains are expressed per unit firing rate (1 = 100 %). PSO-FPID scaling factors: K_e = 0.223 /°C, K_{ec} = 21.5 s/°C, α_p = 0.00, α_i = 0.10, α_d = 0.00.

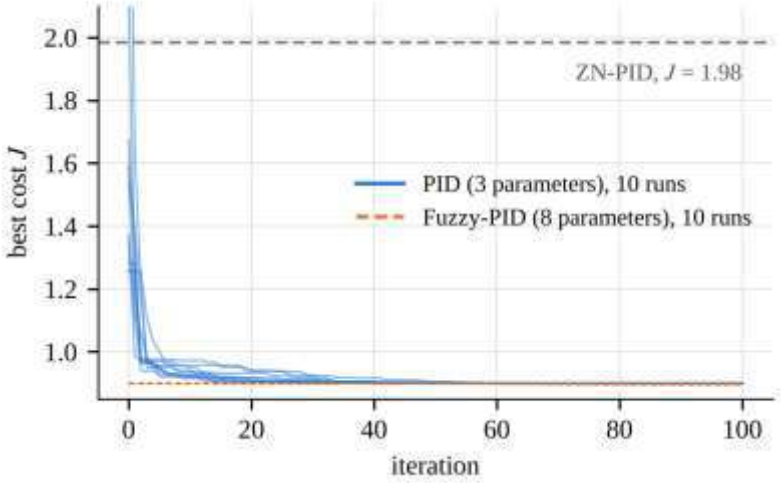

Figure 3. Convergence of the PSO runs. The fuzzy-PID swarms start from the PSO-PID optimum and therefore appear as an almost horizontal line.

Benchmark scenario

Figure 4 shows the benchmark responses and Table 3 the corresponding metrics. During the set-point step all controllers saturate the burner, so the rise time is the same (about 328 s). PSO-PID reduced the overshoot from 0.88 to 0.54 °C and the IAE of the two load disturbances from 203 to 121 °C·s and from 373 to 247 °C·s. The PSO-FPID responses are indistinguishable from those of PSO-PID at the scale of the figure. Measured-flow feedforward lowered the maximum deviation from 0.90 to 0.66 °C for the load increase and from 1.63 to 1.22 °C for the load decrease.

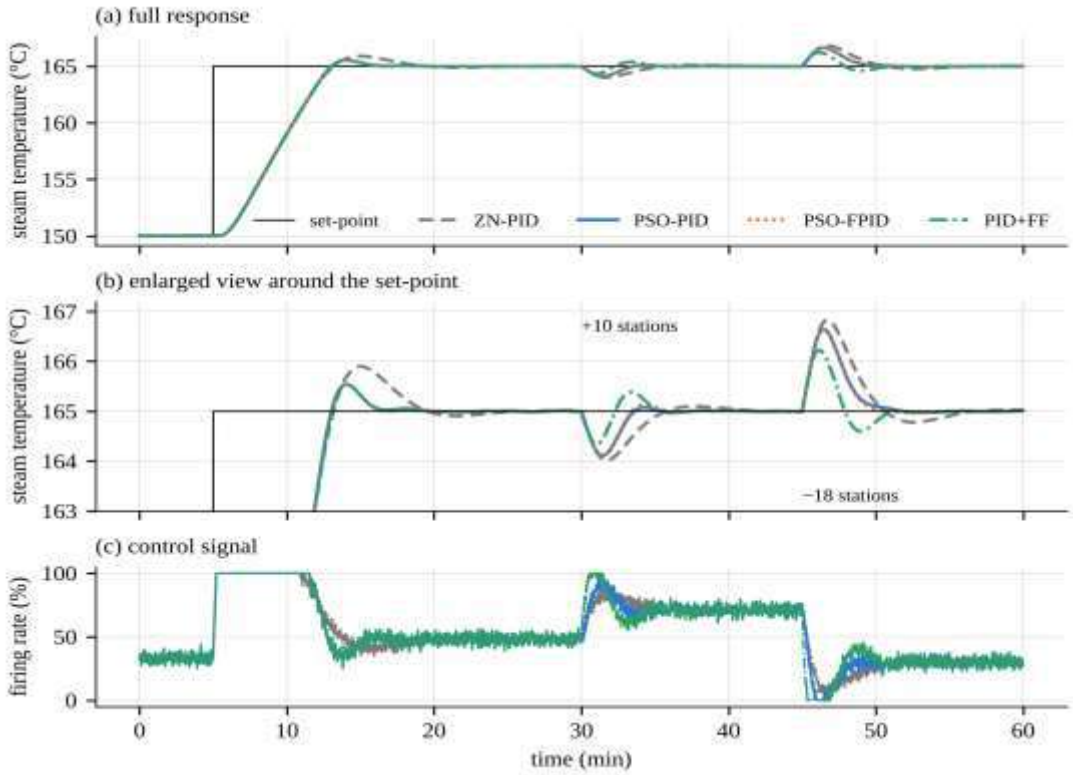

Figure 4. Benchmark scenario: set-point step from 150 to 165 °C at 5 min, load increase of ten stations at 30 min and load decrease of 18 stations at 45 min.

License: This is an open access article under the CC BY 4.0 license: https://creativecommons.org/licenses/by/4.0/

Corresponding Author: Nguyen Thi Lan Huong

Table 3. Benchmark scenario: mean of 20 runs with different measurement-noise sequences.

Controller	Rise time (s)	Over-shoot (°C)	Settling (s)	+10 st.: max dev. (°C)	+10 st.: IAE (°C·s)	+10 st.: recovery (s)	−18 st.: max dev. (°C)	−18 st.: IAE (°C·s)	−18 st.: recovery (s)	TV (–)
ZN-PID	329	0.88	724	0.99	203	210	1.82	373	254	85.7
PSO-PID	327	0.54	548	0.90	121	149	1.63	247	198	92.0
PSO-FPID	327	0.53	547	0.89	123	147	1.63	240	195	92.1
PID+FF	328	0.53	548	0.66	103	95	1.22	176	139	89.6

Rise time: 10–90 % of the step. Settling and recovery: time after which the temperature stays within ±0.5 °C of the set-point. TV: total variation of the firing-rate signal over the whole scenario.

Demand forecasting

Table 4 reports the forecast accuracy on the validation days. For every horizon the network had a lower RMSE than the persistence forecast (the current flow measurement), and the advantage grew with the horizon. The closed-loop MAE was lowest for H = 60 s, which was adopted. On the 20 test days the forecast RMSE at this horizon was 23.5 kg/h, compared with 36.2 kg/h for persistence. Figure 5 shows one test day and the forecast around the morning break.

Table 4. Forecast accuracy and closed-loop error on the ten validation days.

Horizon H (s)	RMSE, persistence (kg/h)	RMSE, ANN (kg/h)	RMSE reduction (%)	Closed-loop MAE (°C)
30	26.6	20.1	24	0.164
45	32.6	22.7	30	0.158
60	37.4	23.9	36	0.154
75	41.5	25.0	40	0.161
90	45.1	25.6	43	0.175

For comparison, the closed-loop MAE on the same days was 0.254 °C for PSO-PID and 0.212 °C for PID+FF.

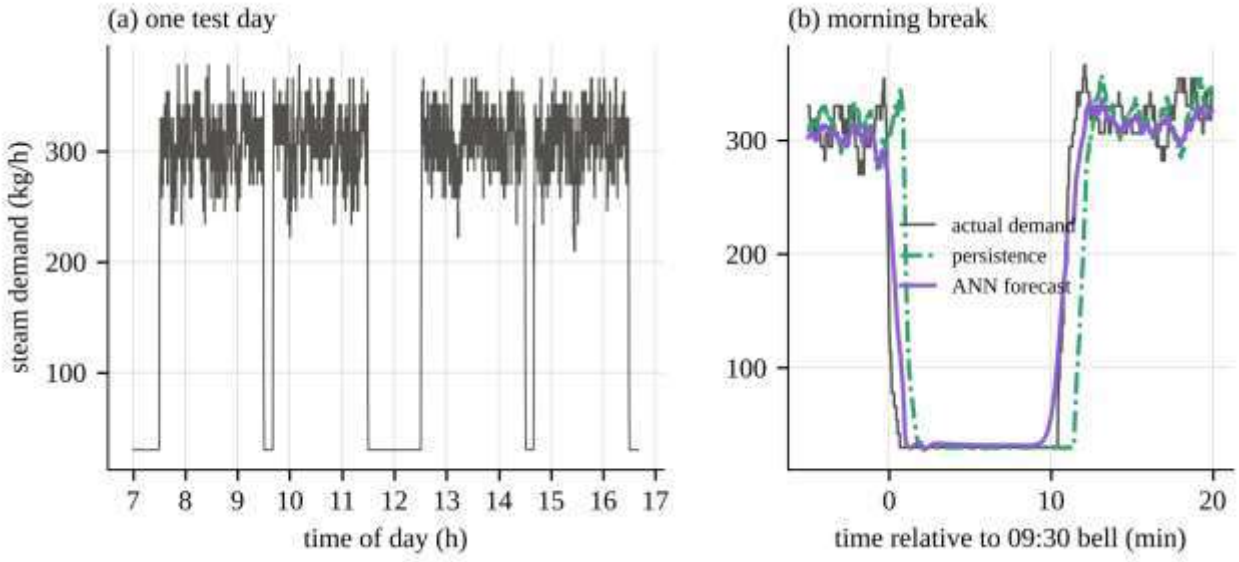

Figure 5. (a) Steam demand on one test day. (b) Demand around the morning break with the 60 s-ahead forecasts plotted at the time they refer to: the persistence forecast is the flow measured 60 s earlier.

Full-shift performance

Table 5 summarises the 20 test days and Figure 6 shows the temperature around the morning break of one of them. With PSO-PID the MAE was 0.244 °C and the largest deviation of the day averaged 2.29 °C. PSO-FPID gave 0.247 °C and 2.30 °C. Measured-flow feedforward gave 0.207 °C and 1.91 °C. The neural feedforward gave 0.148 °C and 0.91 °C and held the temperature within ±0.5 °C for 97.5 % of the shift, against 90.6 % for PSO-PID. All pairwise differences in daily MAE listed in the table were significant (Wilcoxon signed-rank test, $p < 0.001$, $n = 20$), and the ordering of the controllers was the same on every day (Figure 7). Within ±5 min of the bells the MAE was 0.813 °C for PSO-PID, 0.588 °C for PID+FF and 0.221 °C for PID+ANN-FF; outside these windows it was 0.154, 0.147 and 0.137 °C respectively. Daily fuel energy ranged from 1849.9 to 1851.8 kWh across controllers. The total variation of the control signal was 2.4 % higher with the neural feedforward than with PSO-PID.

License: This is an open access article under the CC BY 4.0 license: https://creativecommons.org/licenses/by/4.0/

Table 5. Full-shift performance on the 20 test days (mean ± standard deviation across days).

Controller	MAE (°C)	RMSE (°C)	Max. deviation (°C)	Time within ±0.5 °C (%)	Time within ±1.0 °C (%)	MAE near bells (°C)	MAE elsewhere (°C)	TV (–)	Fuel energy (kWh)
ZN-PID	0.280 ± 0.022	0.534 ± 0.042	2.45 ± 0.15	88.9	92.4	0.984	0.169	920	1849.9
PSO-PID	0.244 ± 0.020	0.462 ± 0.039	2.29 ± 0.15	90.6	93.8	0.813	0.154	1005	1850.8
PSO-FPID	0.247 ± 0.020	0.463 ± 0.039	2.30 ± 0.16	90.6	93.9	0.812	0.158	1006	1850.8
PID+FF	0.207 ± 0.015	0.352 ± 0.030	1.91 ± 0.19	92.3	96.3	0.588	0.147	990	1851.8
PID+ANN-FF	0.148 ± 0.012	0.204 ± 0.019	0.91 ± 0.21	97.5	99.9	0.221	0.137	1030	1850.7

Near bells: within ±5 min of the eight scheduled bells. Fuel energy varies between days by ±113 kWh with the number of staffed stations; the comparison between controllers is paired by day.

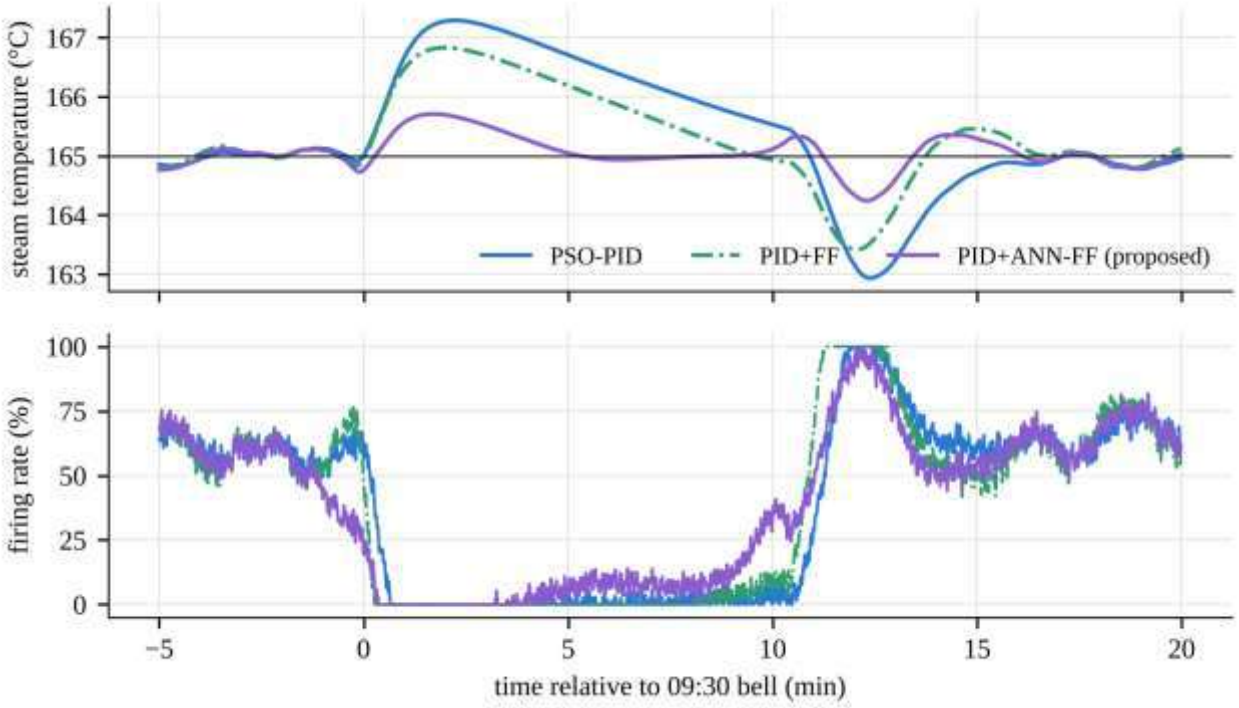

Figure 6. Steam temperature and firing rate around the morning break of one test day.

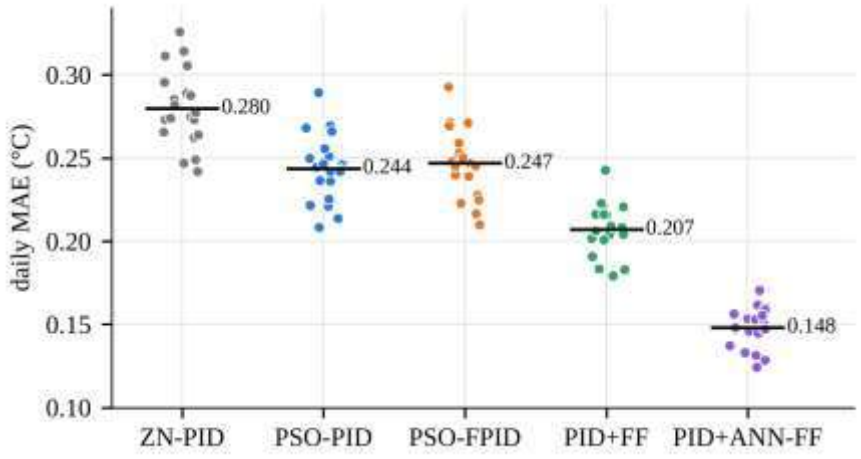

Figure 7. Daily mean absolute error on the 20 test days (one point per day; bars show the mean).

Robustness

Table 6 and Figure 8 give the robustness results. Under plant mismatch the MAE of every controller increased; PID+ANN-FF remained lowest at 0.259 °C against 0.366 °C for PSO-PID, and its maximum deviation was 1.53 °C against 3.15 °C. Under the shifted break, the forecast RMSE rose

License: This is an open access article under the CC BY 4.0 license: https://creativecommons.org/licenses/by/4.0/

Corresponding Author: Nguyen Thi Lan Huong

to 35.8 kg/h, essentially that of persistence (36.0 kg/h). The MAE of PID+ANN-FF rose to 0.176 °C and its maximum deviation to 1.99 °C, which is above that of PID+FF (1.88 °C) and below that of PSO-PID (2.29 °C).

Table 6. Robustness tests on the 20 test days (mean ± standard deviation across days).

Condition	Controller	MAE (°C)	RMSE (°C)	Max. deviation (°C)	Time within ±0.5 °C (%)	Time within ±1.0 °C (%)
Nominal	ZN-PID	0.280 ± 0.022	0.534 ± 0.042	2.45 ± 0.15	88.9	92.4
Nominal	PSO-PID	0.244 ± 0.020	0.462 ± 0.039	2.29 ± 0.15	90.6	93.8
Nominal	PSO-FPID	0.247 ± 0.020	0.463 ± 0.039	2.30 ± 0.16	90.6	93.9
Nominal	PID+FF	0.207 ± 0.015	0.352 ± 0.030	1.91 ± 0.19	92.3	96.3
Nominal	PID+ANN-FF	0.148 ± 0.012	0.204 ± 0.019	0.91 ± 0.21	97.5	99.9
Plant mismatch	ZN-PID	0.367 ± 0.031	0.699 ± 0.059	3.23 ± 0.21	85.2	91.2
Plant mismatch	PSO-PID	0.366 ± 0.028	0.652 ± 0.057	3.15 ± 0.26	83.2	92.0
Plant mismatch	PSO-FPID	0.374 ± 0.029	0.657 ± 0.058	3.17 ± 0.28	82.1	92.0
Plant mismatch	PID+FF	0.345 ± 0.023	0.553 ± 0.047	2.74 ± 0.30	81.1	93.7
Plant mismatch	PID+ANN-FF	0.259 ± 0.020	0.356 ± 0.031	1.53 ± 0.29	86.0	98.4
Break shifted by 5 min	ZN-PID	0.280 ± 0.022	0.533 ± 0.043	2.45 ± 0.17	88.9	92.4
Break shifted by 5 min	PSO-PID	0.243 ± 0.020	0.459 ± 0.042	2.29 ± 0.19	90.7	93.9
Break shifted by 5 min	PSO-FPID	0.246 ± 0.020	0.461 ± 0.043	2.30 ± 0.20	90.6	93.9
Break shifted by 5 min	PID+FF	0.206 ± 0.016	0.349 ± 0.034	1.88 ± 0.21	92.3	96.4
Break shifted by 5 min	PID+ANN-FF	0.176 ± 0.013	0.294 ± 0.026	1.99 ± 0.29	95.3	98.0

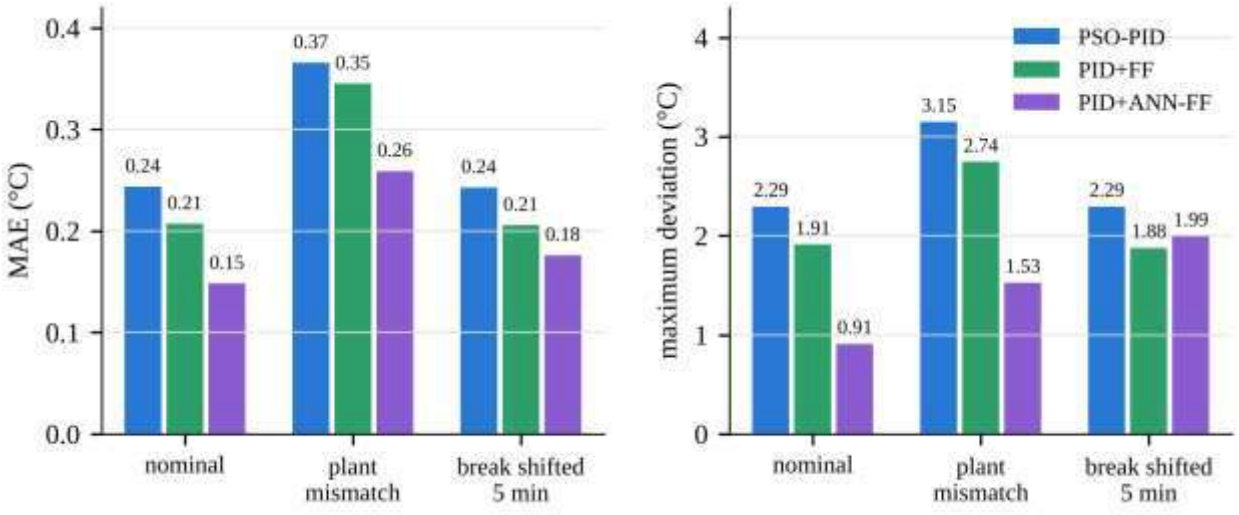

Figure 8. Mean absolute error and maximum deviation under nominal conditions and the two robustness tests (mean of 20 test days).

DISCUSSION

Intelligent feedback tuning

Replacing the Ziegler–Nichols settings by PSO-optimised gains reduced the full-shift MAE by 13 % and cut the integral error after a load step by 34–40 %. This confirms the practical value of metaheuristic tuning reported by Aygun et al. (2012) and Mien et al. (2020), but the improvement is of the size that any careful model-based retuning would be expected to deliver (Skogestad, 2003), and it almost vanished under plant mismatch (0.366 against 0.367 °C). PSO is a convenient way of obtaining good gains from a simulation model; it does not change what a PID controller can do.

The fuzzy self-tuning layer added nothing measurable. Offered the freedom to schedule all three gains, the optimiser switched off the proportional and derivative scheduling and retained only a 10 % modulation of the integral gain, for a 0.6 % reduction of the tuning cost that did not carry over to the test days (0.247 against 0.244 °C). This result differs from much of the fuzzy-PID literature on boilers, and the reason lies in the comparison. In the present plant the ratio of process gain to time constant, which determines the initial slope of the response, is almost independent of load, and the dead time is only 6 % of the time constant. A fixed-gain PID controller is then close to the best that feedback can achieve, and there is little for gain scheduling to exploit. Studies that find large benefits generally concern superheater loops with long, load-dependent dead times, or compare against a Ziegler–Nichols baseline. The finding should therefore not be read as a general statement about fuzzy control, but as evidence that for small saturated-steam boilers a fuzzy supervisory layer is unlikely to repay its commissioning effort.

Forecast-based feedforward

The limiting factor for feedback is visible in Figure 6. After the stop bell the demand falls by more than 250 kg/h in less than a minute, but heat already in the gas path and tube walls continues to reach the water for longer than that, and the temperature overshoots by about 2 °C whatever the

License: This is an open access article under the CC BY 4.0 license: https://creativecommons.org/licenses/by/4.0/

gains. Measured-flow feedforward removes the detection delay and reduced the maximum deviation by 17 %; it cannot remove the actuation lag. The neural forecaster does, for the part of the load that is predictable: it begins lowering the firing rate about a minute before the bell and raising it before work resumes. The benefit is concentrated where it is needed. Around the bells the MAE fell by 73 % relative to PSO-PID, whereas during steady work, when the load varies randomly and cannot be forecast, the three schemes differ by little (0.154, 0.147 and 0.137 °C). The best horizon, 60 s, is close to the apparent dead time of 79 s, which is consistent with the feedforward path needing roughly that long to act.

In information terms, the network contributes little that a fixed schedule could not: it learns the average shape of the transitions and blends it with the current flow. Its practical advantage is that this shape, the ramp rates and their dependence on the number of staffed stations are learned from logged data rather than programmed by hand. Compared with the reinforcement-learning approaches of Zhan et al. (2022), Lee and Jung (2024) and Okafor and Alowaifeer (2025), the scheme is deliberately modest: the learned component only supplies a forecast, the PID loop retains authority and corrects any forecast error, and the network (about 800 weights) is small enough to run in a PLC or an edge device.

Fuel consumption

None of the schemes saved fuel: daily fuel energy differed by about 0.1 % between controllers. This is expected, since the steam demand and the losses fix the heat that must be supplied and the controllers differ only in when they supply it. The case for better temperature control in the ironing room therefore rests on product quality and process stability. An indirect saving is possible if a tighter temperature band allows the set-point, and with it the header pressure, to be lowered, but that effect was not evaluated here and should not be assumed.

Robustness and limitations

The proposed scheme tolerated a substantial mismatch between the plant and the feedforward map: with efficiency 10 % lower and a longer delay, it still halved the maximum deviation relative to PSO-PID, because the integral action absorbs the steady-state error of the map. Its weak point is the timetable. When the break was moved by five minutes without informing the forecaster, forecast accuracy fell to that of persistence and the maximum deviation rose from 0.91 to 1.99 °C, slightly worse than conventional feedforward. The scheme did not become worse than feedback alone, but most of its advantage was lost. A deployed system would need the bell times to be supplied by the factory's scheduling system, or a forecaster that detects the onset of a transition from the flow signal itself.

Several limitations qualify these results. (1) They are obtained entirely by simulation; neither the boiler model nor the demand model has been validated against measurements, and the demand statistics (dwell times, bell jitter, consumption per station) are assumptions. (2) The boiler model is a single lumped energy balance with ideal level control and a fully modulating burner; many small boilers fire solid fuel or operate in on/off or high/low mode, for which the achievable performance is lower. (3) The scheme assumes a steam flow meter, which many small installations lack. (4) Only one fuzzy rule base and one inference type were examined. (5) The forecaster was trained and tested on data from the same generator; real factories have overtime, order changes and seasonal patterns that would require retraining.

CONCLUSION

This study compared five control schemes for the steam temperature of a 500 kg/h fire-tube boiler supplying a 30-station garment ironing line, using a nonlinear simulation model and a stochastic, timetable-driven model of steam demand. Three conclusions follow. First, PSO tuning of the PID gains is worthwhile, reducing the full-shift MAE from 0.280 to 0.244 °C. Second, a PSO-tuned fuzzy self-tuning PID controller offers no advantage over the optimally tuned fixed-gain controller for this lag-dominant plant. Third, a small neural network that forecasts steam demand 60 s ahead from the shift timetable and the measured flow, used as a feedforward signal, reduces the MAE to 0.148 °C (−39 %) and the largest daily deviation from 2.29 to 0.91 °C (−60 %), with unchanged fuel use and 2.4 % more actuator movement. The benefit depends on the timetable being correct.

For practitioners, the implication is that investment in intelligent control of garment-factory boilers is better directed at measuring and anticipating the load than at more elaborate feedback laws. Future work should validate the boiler and demand models with data logged at a garment factory, implement the forecaster on a PLC or edge device and test it on a real boiler, extend the method to on/off and solid-fuel firing, add online detection of timetable deviations, and assess whether tighter control permits a lower steam set-point.

ETHICAL AND COMPLIANCE STATEMENTS

Originality. This manuscript is original work that has not been published or submitted elsewhere.

Conflict of interest. The author should confirm: The author declares no conflict of interest.

Funding. The author should state the funding source, or: This research received no external funding.

Research ethics. The study is based entirely on computer simulation and involved no human participants or animals; ethical approval was not required.

Data and code availability. The simulation code and all numerical results reported in this paper are available from the author on request.

REFERENCES

1) Ait Sahed, O., Kara, K., & Hadjili, M. L. (2015). Constrained fuzzy predictive control using particle swarm optimization. Applied Computational Intelligence and Soft Computing, 2015, 437943. https://doi.org/10.1155/2015/437943
2) Åström, K. J., & Bell, R. D. (2000). Drum-boiler dynamics. Automatica,36(3),363–378.https://doi.org/10.1016/S0005-1098(99)00171-5
3) Åström, K. J., & Hägglund, T. (2006). Advanced PID control. ISA – The Instrumentation, Systems, and Automation Society.
4) Aygun, H., Demirel, H., & Cernat, M. (2012). Control of the bed temperature of a circulating fluidized bed boiler by using particle swarm optimization. Advances in Electrical and Computer Engineering, 12(2), 27–32. https://doi.org/10.4316/AECE.2012.02005
5) Clerc, M., & Kennedy, J. (2002). The particle swarm – explosion, stability, and convergence in a multidimensional complex space. IEEE Transactions on Evolutionary Computation, 6(1), 58–73. https://doi.org/10.1109/4235.985692

License: This is an open access article under the CC BY 4.0 license: https://creativecommons.org/licenses/by/4.0/

6) Geres. (2024). Case study on sustainable energy – Boiler and steam systems: Condensate recovery installation, Chea Sinat Garment Co., Ltd. Switch Garment project, EU SWITCH-Asia Programme. https://www.switch-asia.eu/site/assets/files/4001/case_study_condensate_recovery_chea_sinat_en.pdf
7) Gutiérrez Ortiz, F. J. (2011). Modeling of fire-tube boilers. Applied Thermal Engineering, 31(16), 3463–3478. https://doi.org/10.1016/j.applthermaleng.2011.07.001
8) Hasanbeigi, A., & Price, L. (2012). A review of energy use and energy efficiency technologies for the textile industry. Renewable and Sustainable Energy Reviews, 16(6), 3648–3665. https://doi.org/10.1016/j.rser.2012.03.029
9) He, S.-Z., Tan, S., Xu, F.-L., & Wang, P.-Z. (1993). Fuzzy self-tuning of PID controllers. Fuzzy Sets and Systems, 56(1), 37–46. https://doi.org/10.1016/0165-0114(93)90183-I
10) Kennedy, J., & Eberhart, R. (1995). Particle swarm optimization. In Proceedings of ICNN'95 – International Conference on Neural Networks (Vol. 4, pp. 1942–1948). IEEE. https://doi.org/10.1109/ICNN.1995.488968
11) Kingma, D. P., & Ba, J. (2015). Adam: A method for stochastic optimization. In Proceedings of the 3rd International Conference on Learning Representations (ICLR 2015). https://arxiv.org/abs/1412.6980
12) Lee, C.-M., & Jung, B.-G. (2024). Adaptive control of ships' oil-fired boilers using flame image-based IMC-PID and deep reinforcement learning. Journal of Marine Science and Engineering, 12(9), 1603. https://doi.org/10.3390/jmse12091603
13) Liu, J., Zhang, Z., Zhang, J., & Chen, J. (2024). Application of a neural network on steam drum pressure control in a fixed-bed reactor for exothermic reactions. Applied Sciences, 14(7), 3052. https://doi.org/10.3390/app14073052
14) Mamdani, E. H., & Assilian, S. (1975). An experiment in linguistic synthesis with a fuzzy logic controller. International Journal of Man-Machine Studies, 7(1), 1–13. https://doi.org/10.1016/S0020-7373(75)80002-2
15) Mien, T. L., An, V. V., & Tam, B. T. (2020). A fuzzy-PID controller combined with PSO algorithm for the resistance furnace. Advances in Science, Technology and Engineering Systems Journal, 5(3), 568–575. https://doi.org/10.25046/aj050371
16) Okafor, E., & Alowaifeer, M. (2025). Control optimization of steam boilers via reinforcement learning. IEEE Access, 13, 73146–73160. https://doi.org/10.1109/ACCESS.2025.3563590
17) Pedregosa, F., Varoquaux, G., Gramfort, A., Michel, V., Thirion, B., Grisel, O., Blondel, M., Prettenhofer, P., Weiss, R., Dubourg, V., Vanderplas, J., Passos, A., Cournapeau, D., Brucher, M., Perrot, M., & Duchesnay, É. (2011). Scikit-learn: Machine learning in Python. Journal of Machine Learning Research, 12, 2825–2830.
18) Rumelhart, D. E., Hinton, G. E., & Williams, R. J. (1986). Learning representations by back-propagating errors. Nature, 323(6088), 533–536. https://doi.org/10.1038/323533a0
19) Seborg, D. E., Edgar, T. F., Mellichamp, D. A., & Doyle, F. J., III. (2016). Process dynamics and control (4th ed.). Wiley.
20) Shi, Y., & Eberhart, R. (1998). A modified particle swarm optimizer. In 1998 IEEE International Conference on Evolutionary Computation Proceedings (pp. 69–73). IEEE. https://doi.org/10.1109/ICEC.1998.699146
21) Skogestad, S. (2003). Simple analytic rules for model reduction and PID controller tuning. Journal of Process Control, 13(4), 291–309. https://doi.org/10.1016/S0959-1524(02)00062-8
22) Takagi, T., & Sugeno, M. (1985). Fuzzy identification of systems and its applications to modeling and control. IEEE Transactions on Systems, Man, and Cybernetics, SMC-15(1), 116–132. https://doi.org/10.1109/TSMC.1985.6313399
23) Tognoli, M., Najafi, B., & Rinaldi, F. (2018). Dynamic modelling and optimal sizing of industrial fire-tube boilers for various demand profiles. Applied Thermal Engineering, 132, 341–351. https://doi.org/10.1016/j.applthermaleng.2017.12.082
24) Uddin, M., Bhuiya, K. M. S., Udoy, S. A., Ahmed, M. M., & Hossan, M. N. (2024). Investigation of the energy consumption and emission for a readymade garment production and assessment of the saving potential. Energy Efficiency, 17(8). https://doi.org/10.1007/s12053-024-10281-2
25) UNIDO. (2020). Case study: Lotus Garments, Suez Canal, Egypt – Integration of solar thermal system and heat system optimization. Industrial Energy Accelerator, United Nations Industrial Development Organization. https://www.industrialenergyaccelerator.org/wp-content/uploads/FINAL-12-August-SSO_case-study-Egypt.pdf
26) Wagner, W., & Pruß, A. (2002). The IAPWS formulation 1995 for the thermodynamic properties of ordinary water substance for general and scientific use. Journal of Physical and Chemical Reference Data, 31(2), 387–535. https://doi.org/10.1063/1.1461829
27) Zadeh, L. A. (1965). Fuzzy sets. Information and Control, 8(3), 338–353. https://doi.org/10.1016/S0019-9958(65)90241-X
28) Zhan, X., Xu, H., Zhang, Y., Zhu, X., Yin, H., & Zheng, Y. (2022). DeepThermal: Combustion optimization for thermal power generating units using offline reinforcement learning. Proceedings of the AAAI Conference on Artificial Intelligence, 36(4), 4680–4688. https://doi.org/10.1609/aaai.v36i4.20393
29) Zhao, Z.-Y., Tomizuka, M., & Isaka, S. (1993). Fuzzy gain scheduling of PID controllers. IEEE Transactions on Systems, Man, and Cybernetics, 23(5), 1392–1398. https://doi.org/10.1109/21.260670
30) Ziegler, J. G., & Nichols, N. B. (1942). Optimum settings for automatic controllers. Transactions of the ASME, 64, 759–768.

License: This is an open access article under the CC BY 4.0 license: https://creativecommons.org/licenses/by/4.0/

Corresponding Author: Nguyen Thi Lan Huong